The earliest securely-dated hominin artefact in Anatolia?

D. Maddy [a, *], D. Schreve [b], T. Demir [c], A. Veldkamp [d], J.R. Wijbrans [e], W. van Gorp [f],
D.J.J. van Hinsbergen [g], M.J. Dekkers [g], R. Scaife [h], J.M. Schoorl [f], C. Stemerdink [a],
T. van der Schriek [a]

[a] School of GPS, Newcastle University, Newcastle upon Tyne NE1 7RU, UK
[b] Department of Geography, Royal Holloway University of London, Egham TW20 0EX, UK
[c] Department of Geography, Harran University, 63300 Sanliurfa, Turkey
[d] Faculty of Geo-Information Science and Earth Observation (ITC), Twente University, Enschede, The Netherlands
[e] Department of Earth Science, VU University, De Boelelaan 1085, 1081 HV Amsterdam, The Netherlands
[f] Soil Geography and Landscape Group, Wageningen University, 6700 AA Wageningen, The Netherlands
[g] Department of Earth Sciences, Utrecht University, Budapestlaan 4, 3584 CD Utrecht, The Netherlands
[h] School of Geography, University of Southampton, Southampton SO17 1BJ, UK

ARTICLE INFO

ABSTRACT

Anatolia lies at the gateway from Asia into Europe and has frequently been favoured as a route for Early Pleistocene hominin dispersal. Although early hominins are known to have occupied Turkey, with numerous finds of Lower Palaeolithic artefacts documented, the chronology of their dispersal has little reliable stratigraphical or geochronological constraint, sites are rare, and the region's hominin history remains poorly understood as a result. Here, we present a Palaeolithic artefact, a hard-hammer flake, from fluvial sediments associated with the Early Pleistocene Gediz River of Western Turkey. This previously documented buried river terrace sequence provides a clear stratigraphical context for the find and affords opportunities for independent age estimation using the numerous basaltic lava flows that emanated from nearby volcanic necks and aperiodically encroached onto the contemporary valley floors. New $^{40}Ar/^{39}Ar$ age estimates from these flows are reported here which, together with palaeomagnetic measurements, allow a tightly-constrained chronology for the artefact-bearing sediments to be established. These results suggest that hominin occupation of the valley occurred within a time period spanning ~1.24 Ma to ~1.17 Ma, making this the earliest, securely-dated, record of hominin occupation in Anatolia.

1. Introduction

The Anatolian peninsula, bounded by the Black Sea to the north, the Aegean Sea to the west, and the Mediterranean Sea to the south, forms the western limit of Asia and, albeit still within modern Turkey, shares a border with European Eastern Thrace to the west (Fig. 1). This pathway from Asia into Europe has frequently been proposed as a route for Early Pleistocene hominin dispersal (Dennell, 2003, 2008) but the timing of this dispersal remains poorly understood (Bar-Yosef and Belmaker, 2011). Within Turkey, the oldest known hominin locality is that of Kocabaş, in the Büyük Menderes valley in Western Anatolia (Fig. 1), where

fragments of a cranium, tentatively attributed to *Homo erectus*, have been found in travertine deposits (Kappelman et al., 2008). Although Kappelman et al. (2008) reported an age of 490–510 ka based upon thermoluminescence results, a revised age estimate of between 1.3 and 1.1 Ma has recently been suggested on the basis of magnetic polarity measurements and modelled $^{26}Al/^{10}Be$ cosmogenic isotope burial age determinations from sediments that lie below and above the inferred hominin-bearing Upper Travertine (Lebatard et al., 2014, p10). Elsewhere, evidence for human occupation is limited to isolated finds of Lower Palaeolithic stone tools (Harmankaya and Tanındı, 1996), yet the chronology of hominin dispersal across Anatolia has, to date, had little reliable stratigraphical or geochronological constraint (Kuhn, 2002, 2010). This stems from a scarcity of detailed description of, and substantive geochronological constraint on, Plio-Pleistocene sequences within Turkey.

* Corresponding author.
  E-mail address: darrel.maddy@ncl.ac.uk (D. Maddy).
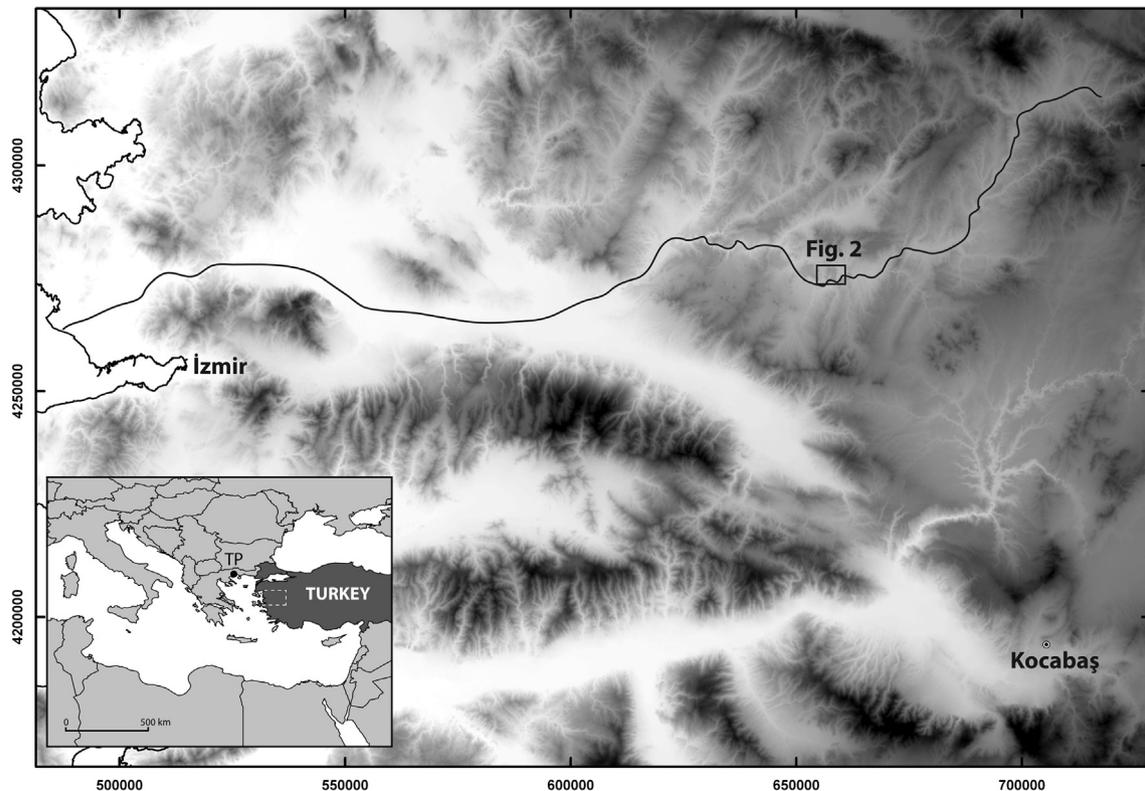
Fig. 1. Location of the Gediz River, Western Anatolia. Location of the Gediz River plotted on the global ASTER Global Digital Elevation Model v2 (GDEM; ASTER GDEM is a product of METI and NASA) with the study area indicated. Inset shows the wider setting of the study area with the Mediterranean together with the location of the Tenaghi Philippon site (TP) discussed in the text. The grid is UTM Zone 35S.

One such sequence, the Early Pleistocene sedimentary sequence of the Gediz River valley around Kula (Figs. 1 and 2), has, however, recently been the subject of extensive studies (Maddy et al., 2005, 2012a). These studies describe a staircase of 11 river terraces from T11 (highest and oldest) to T1 (lowest and youngest), cut at progressively lower levels into the underlying Miocene Ahmetler Formation (Ersoy et al., 2010). The terrace deposits are ancestral floodplains of the Gediz River, which flows from east to west, with progressive incision driven both by fluvial system adjustment to the on-going uplift and by climate-driven hydrological/vegetation change. The detailed stratigraphy is complex, with the terraces often dissected by the deposits of northerly-derived tributaries diverted by lava incursions (Maddy et al., 2012b). Critically, however, the fluvial deposits of the Gediz River and its tributaries from this sequence are capped by basalts that allow the terrace sequence to be assigned an Early Pleistocene age on the basis of a limited number of previously published K/Ar age estimates (Westaway et al., 2004, 2006).

The most extensive exposures in this sequence lie beneath the lavas that form the Burgaz Plateau (Fig. 2). Here, the onset of volcanism is penecontemporaneous with a Gediz valley floor at the T6 level and all lavas appear to emanate from the same Burgaz Bağtepe volcanic neck. Episodic eruptions from this neck continued during the time period represented by the sediments underlying T5–T1. Following the final blockage of the valley floor in this area by the lavas that cap T1 on Kale Tepe, the Gediz River was diverted northwards at the upstream end of the blockage, forming a meander loop that returned to the pre-blockage valley floor downstream of the Kale Tepe lava dam, leaving Kale Tepe to occupy the meander core.

In this paper we report the find of an artefact from within the fluvial/alluvial sediments lying in the palaeomeander section. In addition, we establish the time period during which the palaeomeander loop was occupied by the Gediz, and from that infer the likely period of hominin occupation. Currently there are five published age estimates for the Burgaz plateau lavas recorded in the literature. The first reported age estimate, which lacks precise location, was 1100 ka (Borsi et al., 1972). Two estimates of 1370 ± 100 and 1120 ± 60 ka are recorded from close to the Burgaz Bağtepe neck (Richardson-Bunbury, 1996, Fig. 2α) and estimates of 1031 ± 12 and 996 ± 12 ka are suggested for a lava north of Burgaz village (Westaway et al., 2006, Fig. 2β). However, none of these existing age estimates relate directly to the underlying river terrace record or the palaeomeander sequence. Thus, in an attempt to constrain the age of hominin occupation of the palaeomeander and the age of the terrace record buried beneath the plateau, we have sampled a number of lavas (Fig. 2A–G) for age estimation and, as part of a wider programme, performed palaeomagnetic measurements to determine the magnetic polarity during eruption.

2. Methods

2.1. Lithostratigraphy

Standard sedimentary logging procedures were deployed to establish the stratigraphy of the artefact-bearing palaeomeander infill sequence. Sediment outcrops, exposed along the eroded edges of the lavas that form the Burgaz plateau, were logged in detail using standard lithofacies descriptors and, where possible, scaled face sections were drawn in the field in order to establish sedimentary architecture. Bounding surface heights were acquired using a Sokkia 4c Total Station. Sections located in positions too hazardous for safe reflector positioning have lower precision heights obtained using a laser range finder. Logged sections,
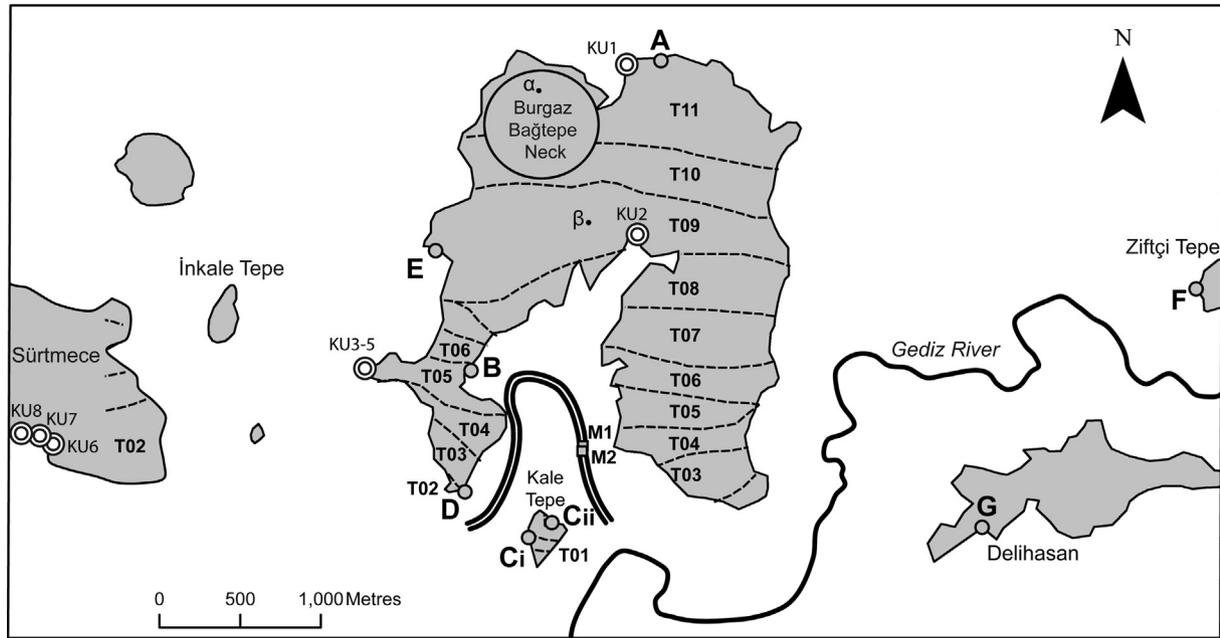
Fig. 2. General map of the study area showing the presumed extent of the sub-basalt Gediz terraces (T1–T11, after Maddy et al., 2012) and the route of the incised meander section. A–G show the location of basalts samples for ^{40}Ar/^{39}Ar analysis. KU1–KU5 shows the sampling positions of lava used in palaeomagnetic measurements.

together with more continuous field observations, are used to determine significant stratigraphical units (U1-6, Fig. 3) which comprise related sedimentary facies.

2.2. Ar/Ar sampling and procedures

Lava samples, taken from stratigraphically significant locations (Fig. 2A–E), were collected for ^{40}Ar/^{39}Ar radio-isotopic age estimation. Incremental heating experiments were carried out at the VU University, Amsterdam. Groundmass separates were prepared following established methodology and focussed on obtaining

homogenous fragments of microcrystalline groundmass to minimize the chance of inherited argon present in phenocryst phases. Groundmass samples (~500–700 mg) were packed in 20 mm diameter Al-foil packages, together with 9 mm diameter packages containing mineral standard DRA-1 sanidine. This standard has a recalculated K/Ar age of 25.45 Ma (Wijbrans et al., 1995; Kuiper et al., 2008). Sample containers were packed in a standard Al-irradiation capsule and irradiated for 1 h in a Cd-lined rotating facility (RODEO) at the Petten High Flux Reactor in The Netherlands. After their return, samples were loaded onto a 65-mm sample tray with 5 machined depressions of 3 mm deep and 17 mm wide and
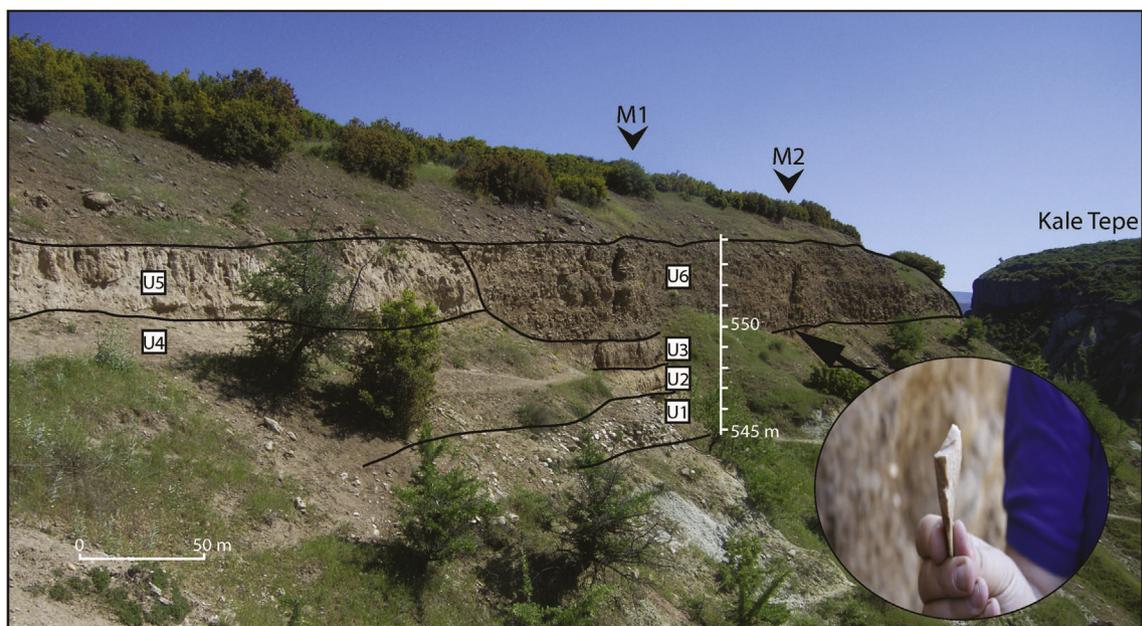
Fig. 3. Photograph of the main eastern (upstream) palaeomeander outcrop. Approximate bounding surfaces delimit six Pleistocene units (U1-6) overlying the Miocene Ahmetler Formation. Section located beneath M1 and M2 are discussed in the text. Inset shows a close-up of the hard hammer flake observed within the M2 section.

placed in a vacuum house with a 50 mm diameter multispectral ZnS window. Incremental heating was done by defocusing a CO_2 laser beam to a *ca* 2 mm straight bar using an industrial scanhead with a triangular deflection current of 200 Hz frequency. Samples were evenly heated by applying a fine x–y raster pattern over each of the sample positions. Measurements were done using a quadrupole mass spectrometer (Schneider et al., 2009). Mass spectrometer runs consist of stepwise measurement of the argon mass spectrum from m/e 36 to m/e 40, where on m/e 36, 39 and 40 seven readings were taken at 0.05 m/e intervals on the flat peak top, and for m/e 37 and 38 one single reading was taken. The baseline was measured at m/e 35.45. Beam signals for all peaks were measured using a pulse counting SEM detector. Aliquots of air are measured routinely during the measurement programme to monitor mass discrimination (Wijbrans et al., 2011).

2.3. Palaeomagnetic sampling and procedures

We collected 35 samples from 5 lava sites (Fig. 2 KU1–KU5) on the Burgaz plateau and a further 21 samples from 3 lava sites on Sürtmece (Sarniç Plateau, KU6–KU8, Fig. 2). Samples were extracted using a water-cooled, gasoline-powered, motor drill. They were oriented with a magnetic compass and all magnetic measurements were corrected for the present-day declination of ~4°. All samples were demagnetized using alternating field (AF) progressive demagnetizations with 5–10 mT increments up to 100 mT. The natural remanent magnetization (NRM) of the specimens was measured on a 2G Enterprises horizontal DC SQUID magnetometer (noise level $3 \times 10{-}12$ Am^2), interfaced with an in-house developed robot-assisted automated measuring device at the Paleomagnetic Laboratory 'Fort Hoofddijk' of Utrecht University. Demagnetization diagrams of the NRM were plotted in orthogonal vector diagrams (Zijderveld, 1967). In addition, a number of multi-component samples were plotted on equal-area projections. Initial NRM intensities typically range from 0.5 to 2.0 A/m, at the upper end of the dynamic range of the instrument. When vector end-points showed a trend towards the origin of the diagram, we determined this component to be the characteristic remanent magnetization (ChRM). ChRM's were calculated with principal component analysis (Kirschvink, 1980). Because the samples plateaus are prone to lightning strikes, which create magnetic overprints, samples were collected over an area of several tens of square meters to increase the chance that lightning-induced overprints have different directions in different samples. Where a magnetic overprint led to overlapping demagnetization spectra between two components we used the great-circle approach of McFadden and McElhinny (1988) to resolve the ChRM direction from the great circles defined by the two components for individual specimens from the same site. If the overprint direction is not everywhere the same, the ChRM direction can be deduced by the common intersection point of all great circles obtained from a lava site, with two solutions (one normal, one reversed), whereby the polarity is determined by non- or only weakly overprinted samples within the same site. Geomagnetic polarities indicated by the ChRM directions were interpreted with respect to the geomagnetic polarity timescale (APTS 2012: Hilgen et al., 2012).

3. Results

3.1. Lithostratigraphy and the Palaeolithic artefact

The route of the palaeomeander is identified from a laterally continuous sequence of coarse-medium gravels (U1, Fig. 3), overlain in places by alluvial sands and silts (U2 and U3, Fig. 3). These deposits are up to 2 m thick on the eastern, upstream, limb of the

palaeomeander, but are thinner, and more discontinuous, on the downstream western limb. In all outcrops, the fluvial deposits lie beneath up to 8 m of non-fluviatile sediments, which form the infill of the palaeomeander post-abandonment by the Gediz. The gravels can readily be distinguished from earlier Gediz gravels (T1–11) on the basis of their high basalt clast content (>10%), which reflects erosion of the adjacent lava dam by a diverted Gediz River. The gravels, which represent in-channel sediments, are, in places, overlain by finer alluvial (over-bank) sediments, suggesting migration of the channel within the meander section with occasional inundation of a narrow adjacent floodplain. These overbank sediments display two weakly-developed palaeosols at location M1 (Figs. 2 and 3), which suggests periods of reduced flood frequency, allowing pedogenesis on the adjacent floodplain.

The palaeomeander cuts into an area located between the lavas that form the western and eastern arms of the Burgaz Plateau (Fig. 2) and lies on a flat surface incised through the terrace sequence, directly cut into the underlying Miocene basin fill sediments. This surface, lying at ~545 m above sea level, is within the elevation range of the sediments that form the T1 terrace (540–550 m, Maddy et al., 2012a) on Kale Tepe. It therefore seems likely that the formation of the meander loop results from diversion of the Gediz as a response to the blockages of the T1 valley floor by the lavas capping Kale Tepe. The preserved sequence records the last position of this diverted route prior to abandonment and is therefore younger than the basalt dam. Thus the age of the Kale Tepe dam would provide a maximum age for the sediments occupying the palaeomeander.

The infill sediments, overlying the fluviatile sequence in the palaeomeander, provide some indications of the likely reasons for abandonment. Immediately overlying the fluvial and alluvial deposits, where not removed by later erosion, is a thick (up to 4 m) sequence of calcareous sands fining upwards to silts and clays (U4, U5 Fig. 3). These sediments were deposited in a low-energy, standing water environment. Towards the top of the sequence, lenticular clusters of basaltic cobbles suggest aperiodic slumping of upslope materials into this standing water body. The lateral and vertical extent of this unit suggests this is unlikely to be the simple infill of an abandoned channel i.e. an oxbow lake infill; more likely these sediments were laid down in a deeper water body, a lake formed in response to the downstream damming of the river. These lake sediments are cross-cut by thick sequences of sub-aerially deposited slope sediments (U6, Fig. 3) that include discrete coarse landslides with basaltic boulders up to 3 m in diameter, and an apron of crudely stratified mass movement deposits composed of weathered basalt derived from the lava flow upslope. There is no evidence to suggest the presence of the Gediz River within the palaeomeander section after the formation of the lake. The age of the downstream blockage of the river would thus constrain a minimum age for the sediments occupying the palaeomeander.

During our 2005 field-season, we observed a quartzitic artefact immediately below the upper bounding surface of, and thus within, an alluvial sequence (U3, Fig. 3) overlain directly by slope-derived materials at M2 (U6, Figs. 2 and 3). The artefact was removed from the section only to facilitate a sketch and photographic record and was then replaced as required by visa restrictions. The artefact (inferred to be a hard hammer product) has a visible striking platform and a clearly-developed bulb of percussion with minor stress fissuring on the proximal ventral surface (Fig. 4a). There is evidence for at least two prior removals on the dorsal surface, including one flake scar terminating in a hinge fracture (Fig. 4b). The presence of at least two removals makes it highly unlikely that this results from natural processes. Although the gravels of U1, along with those from the higher terrace sequence, contain large quartzitic clasts, these tend to display flat fractures and despite the

counting and identification of thousands of clasts from these and similarly-derived gravels, we have not observed any comparable clasts within the Lower Pleistocene sequence. Furthermore, it is widely accepted that flake-mimicking humanly-struck material can only be convincingly generated in high energy environments e.g. beaches (Bridgland et al., 1997). None of the sediments in this sequence represent high energy transport. Even the overlying slope sediment, which is composed almost entirely of basalt, results from depositional processes associated with low angle slides along weak shallow failure planes within the underlying Miocene Ahmetler Formation, together with less abrupt low energy mass movements. Thus, the occurrence of this flake within the fine-grained alluvial sequence is distinctive and unusual and its form is highly unlikely to have resulted from natural erosion processes.

The dimensions of the flake were 56 mm from the platform to the distal end and 44 mm across the maximum width. There is no suggestion that this artefact has been transported by the river, since the flaking features are clear and quartzitic artefacts are notoriously difficult to identify when rolled and abraded (Wymer, 1999); more likely it indicates the presence of hominins on the floodplain of the Gediz within the meander section. Constraining the occupation of the meander by the Gediz thus provides geochronological constraint for the occupation.

3.2. Geochronology

Our new age estimation data (Table 1, Fig. 5c) provide a tight chronology for these events. Conventionally, a groundmass plateau age estimate is considered acceptable if a well-defined age plateau exists at 1σ with mean square weighted deviation (MSWD) values close to 1 calculated for the steps included in the plateau, and consisting of three or more contiguous steps which contain 50% or more of the ^{39}Ar released. Furthermore, isochron ages should agree with the plateau ages within analytical error, and $^{40}Ar/^{36}Ar$ intercepts derived from regression analysis should not be significantly different from the atmospheric level of 298.56 (Lee et al., 2006). Although samples Ci, Cii, D and G failed to meet these criteria in full, all age estimates presented here are considered to be

of sufficient quality (for detailed analysis and discussion see supplemental data S1/S2).

Geochemical analysis (see supplemental data S1 for details) of samples Ci and Cii classifies both samples as tephrite or basanite. They have similar SiO_2, $Na_2O + K_2O$ and trace element values and displayed similar K/Ca ratio patterns throughout the incremental heating experiments. As both samples were taken from a lava covering T1 on Kale Tepe, their similar chemistry may suggest they are samples from the same flow unit. This flow unit would have dammed the Gediz River and thus triggered the diversion of the river into the meander loop. To increase the precision of the age estimates, these samples were therefore combined to give an age estimate from two samples of 1255.8 ± 16 ka (Table 1, C). Similarly, the basal lava covering the western arm of Burgaz (location D) has a combined age estimate from two samples of 1241.1 ± 9.3 ka. The geochemistry of these flow units, similarly classified as tephrite or basanite, suggests they are closely related to the lava covering Kale Tepe and thus these estimates (C and D) can themselves be combined to give our best age estimate for this lava of 1246.6 ± 8.2 ka. The problems with these samples identified above suggest, however, that this combined estimate is likely to slightly overestimate the true age: we thus conclude that the palaeomeander section is likely to be no older than ~1.24 Ma.

Establishing an age for the damming event that led to the abandonment of the palaeomeander is more difficult but the data suggest that one flow unit is younger than the Kale Tepe lava. Lava at location E has an age estimate of 1170.2 ± 9.7 ka. This lava is considered to be the up-flow remnant of a flow unit that extended south-westwards onto Sürtmece at the south-eastern extremity of the Sarnıç Plateau (Fig. 2), where it has a base which falls slightly beneath the level of a projected T1 profile (Maddy et al., 2012a). This lava would have blocked the contemporary Gediz valley floor and caused the palaeomeander section to become flooded. It remains possible, however, that an earlier lava dam may have caused the palaeomeander to be abandoned and thus the ~1.17 Ma age estimate represents a minimum age for meander flooding and abandonment.
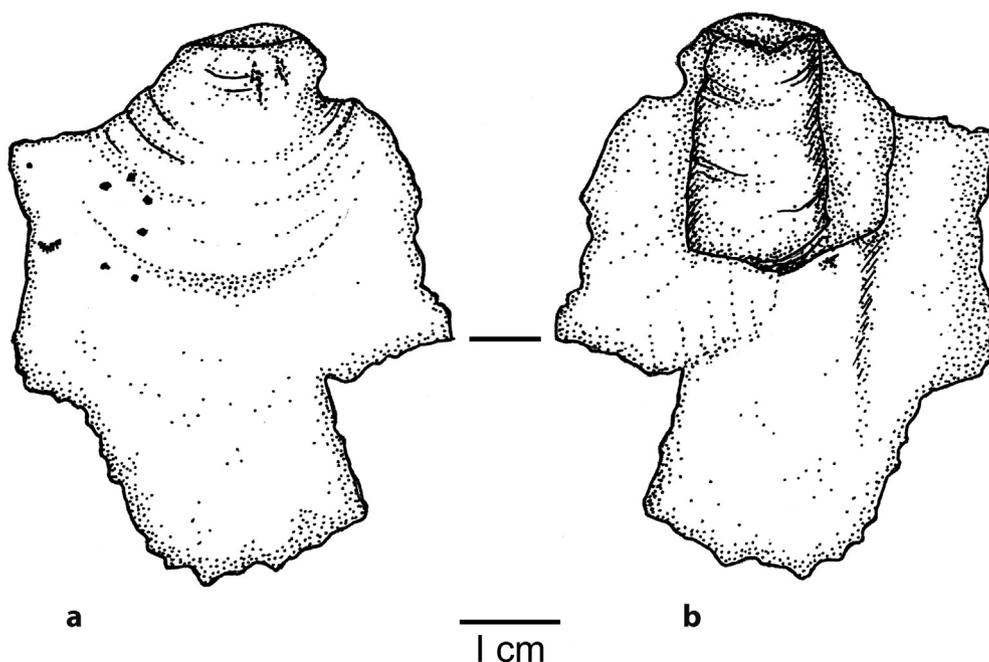

Fig. 4. a. Ventral and b. Dorsal sketch of the artefact recovered from the upper part of U3 at location M2 (Figs. 2 and 3).

Table 1
Summary of $^{40}Ar/^{39}Ar$ analyses.

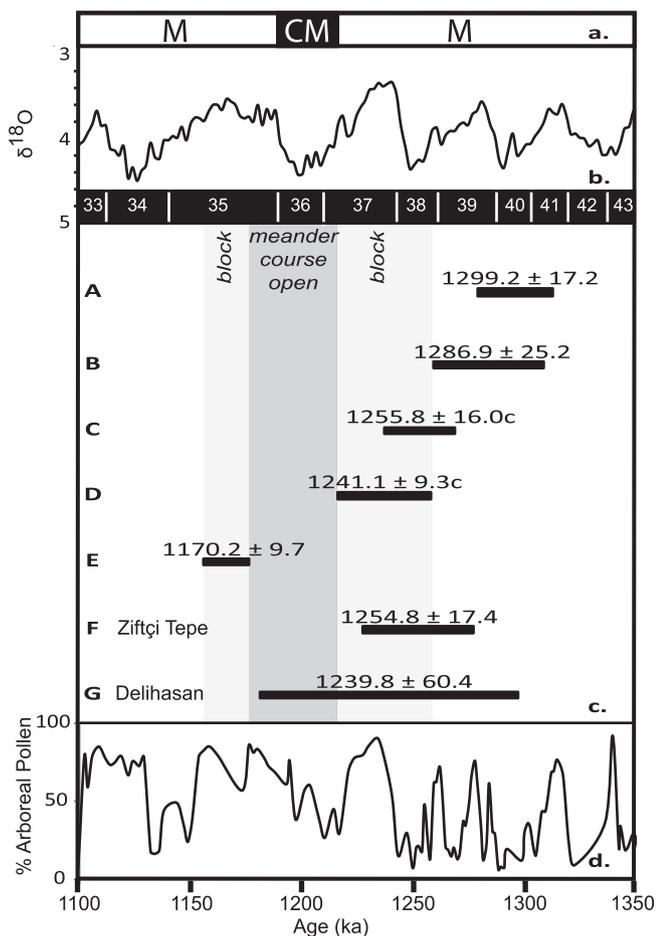| Name	Sample	Labcode	Plateau age (ka)	1σ	MSWD	N. Isochron age (ka)	1σ	Inv. Isochron age (ka)	1σ
A	03E Burgaz No (above 47)	VU87 WG3_A2	1299.2	17.2	0.50	1288.3	22.1	1290.9	22.0
B	02R Burgaz west	VU87 WG2_B1	1286.9	25.2	0.71	1277.5	27.0	1280.9	27.2
Ci	W6_K2	VU94 W6_1_B1	1265.9	17.8	1.57	1180.8	53.3	1181.4	53.1
Cii	03c Kale Tepe	VU87 WG3_B1	1251.0	25.2	6.28	1263.2	29.7	1263.9	29.4
C	Ci and Cii combined	–	1255.8	16.0	3.73	1258.8	23.0	1259.7	22.5
D	W4_BW1	VU94 W4_1_C2/VU94W5_2_B3	1241.1	9.3	1.90	1214.1	13.4	1217.0	12.7
	C and D combined	–	1246.6	8.2	2.61	1239.4	10.6	1242.2	10.4
E	W11_BW2	VU94 W11_1_B1	1170.2	9.7	0.62	1163.8	20.6	1166.0	20.3
F	GB2 Ziftce	VU87 WG2_B3	1254.8	17.4	1.26	1242.4	18.6	1249.4	19.2
G	GB4 Delihasan	VU87 WG2_A2	1239.8	60.4	0.62	1235.2	145.1	1234.2	139.4

3.3. Palaeomagnetism

Demagnetization diagrams typically demonstrate the presence of one magnetic component that decays towards the origin. Initial magnetic intensities were very high, between 1 and 75 A/m, as expected for basaltic lavas. Typical demagnetization diagrams are given in Supplemental S3 and site average directions and statistical parameters are given in Table 2. Many samples experienced gyroremanent magnetization at demagnetization steps beyond

Fig. 5. Results from the Ar–Ar analyses set within a wider framework of climate and environmental change. **a**. Palaeomagnetic timescale. M is Matuyama reversed Chron, CM is Cobb Mountain normal Event (Hilgen et al., 2012). **b**. LR04 stacked δ^{18}O record (Lisiecki and Raymo, 2005). MIS are shown based upon the LR04 age model. **c**. Plateau ages for the seven sample locations shown in Fig. 2. **d**. Vegetation recorded (changing proportions of tree taxa) at Tenaghi Philippon, Greece (see Fig. 1 TP, Tzedakis et al., 2006).

25–30 mT (Dankers and Zijderveld, 1981). This did not influence the determination of the magnetic polarity, and where demagnetization steps below 30 mT typically already converged towards the origin, and were consequently interpreted as the ChRM without applying great-circle analysis. Some samples of sites KU1, 3, 4, 6, and 7 clearly showed two simultaneously decaying components, one with varying orientations (likely because of lightning) and one common among all samples. The common component was found using great-circle analysis of McFadden and McElhinny (1988).

Averages and statistical parameters of each lava site were determined by Fisher (1953) statistics. All lava sites, except KU 5, have a Fisher precision parameter k well exceeding 50 (Table 2), which is normally taken as the lower-bound cut-off value for a reliable spot reading of the geomagnetic field (Biggin et al., 2008; Johnson et al., 2008). All sites, except KU5, yielded unequivocal reversed polarities (Table 2, supplemental S3). The seven samples of site KU 5 yielded two normal, two reversed, and three multi-component directions that span great-circles. Since the samples were taken from a single flow unit, this indicates that either the normal or reversed directions are overprint directions. There is no straightforward explanation for this result, but the site does not allow a conclusive polarity interpretation. Since lavas cool very quickly, they record a spot reading of the paleomagnetic field direction, which underwent palaeo-secular variation. As a result of such short-term magnetic field direction variations, the directions measured in a single lava site may deviate up to ~25° from the palaeomagnetic pole. All sites yield declinations that are deviating clockwise from the south pole. It is important to note that particularly the sites from the Burgaz plateau are very tightly clustered, and do not average palaeo-secular variation (Deenen et al., 2011). The declination should therefore not be interpreted as the result of a tectonic rotation.

The reversed polarities are in agreement with the new geochronology. All lavas sampled on the Burgaz plateau are thus placed within the Matuyama chron (Fig. 5a) and in light of the new Ar/Ar data it is likely that all pre-date the Jaramillo normal subchron (~0.99–1.07 Ma, spanning across MIS 31–27) and none originate in the brief normal Cobb Mountain Event (~1.19–1.22 Ma, spanning from late MIS 37 to the MIS 36/35 boundary). On this basis it is likely that the lavas that predate the meander, pre-date the Cobb-Mountain Event. Significantly, however, the lava at location E is the probable up-flow equivalent of at least one of those which was sampled on Sürtmece (KU6–KU8, see Maddy et al., 2012). Thus lava at location E, with an age estimate of 1170.2 ± 9.7 ka, most likely postdates the Cobb Mountain Event.

4. Discussion and conclusion

The suggested presence of hominins between ~1.24 and ~1.17 Ma is significant. Specifically, these data tend to support the older chronology for the Kocabaş skull (Lebatard et al., 2014).

Table 2
Summary of palaeomagnetic results and directional statistics of the 5 sites located on the Burgaz and Sarniç plateaus (Fig. 2). Lat = latitude of the site; Lon = longitude of the site; Type indicates 'gc' when the site average was constructed using the great circle method of McFadden and McElhinny (1988), as well as the number of great circles used. The remaining samples are regular ChRM's determined using the Kirschvink (1980) procedures; Na = number of samples analysed; Nc = number of samples used to construct the site average; D = declination; I = inclination; k = Fisher (1953) precision parameter for the site; α95 = 95% confidence limit of the site. Directions are in in situ coordinates; subordinate bedding dips of a few degrees of the plateau lavas are interpreted as non-tectonic, primary tilts. Group means per plateau are indicated in italic font.

Site	Lat	Lon	Type	Na	Nc	D	I	k	α95	Polarity
Burgaz plateau				*5*	*4*	*211.1*	*−68.7*	*1523.2*	*2.4*	*Reversed*
KU 1	38.6301	28.8128	gc (4)	7	7	214.9	−69.2	90.5	6.4	Reversed
KU 2	38.6199	28.8133		7	6	214.0	−69.7	1446.2	1.8	Reversed
KU 3	38.6129	28.7943	gc (5)	7	6	211.8	−67.3	741.9	2.5	Reversed
KU 4	38.6129	28.7943	gc (2)	7	6	204.1	−68.3	98.9	6.8	Reversed
KU 5	38.6129	28.7943		7	0	Inconclusive: both normal and reversed. See text				
Sarniç plateau				*3*	*3*	*199.6*	*−59.6*	*32.4*	*22.0*	*Reversed*
KU 6	38.6103	28.7717	gc (2)	7	5	209.0	−69.8	108.2	7.4	Reversed
KU 7	38.6102	28.7697	gc (7)	7	7	191.1	−44.3	810.1	1.9	Reversed
KU 8	38.6353	28.7660		7	7	206.1	−63.8	71.3	7.2	Reversed

Despite the stratigraphical uncertainty caused by the cosmogenic isotope geochronology sampling being performed many years after the bones were recovered, a problem acknowledged by Lebatard et al. (2014), our results suggest that hominins were indeed present in western Anatolia during this time interval.

Elsewhere in Turkey, only two localities have so far yielded artefacts with independent age control and both are comparatively insecure. A small lithic assemblage from a fossiliferous lignite at Dursunlu quarry 60 km northwest of Konya (Güleç et al., 1999) has been attributed, on the basis of reversed palaeomagnetic measurements, to the Matuyama chron after the Jaramillo (i.e. between 0.78 and 0.99 Ma). However, palaeontological evidence from this locality has recently been used to extend this timescale, possibly back to 1.1 Ma (Güleç et al., 2009). The Gediz flake reported here compares well to the small core and flake industry suggested for Dursunlu, where the artefacts are made of quartz, with rare pieces of flint and an igneous rock. At Kaletepe Deresi 3, located 200 km east of Dursunlu, Acheulean artefacts have been reported from deposits overlying rhyolitic bedrock that has age estimates spanning 1.3—1.1 Ma (Slimak et al., 2008).

In the wider region, the oldest archaeological site in southwestern Asia is Dmanisi in Georgia, dating to ~1.8 Ma (Gabunia and Vekua, 1995; Gabunia et al., 2000; Ferring et al., 2011; Messager et al., 2011). Here, remains of *Homo*, recently attributed to *H. erectus ergaster georgicus* (Lordkipanidze et al., 2013) are found in association with a 'Mode 1' flake and core industry and a mammalian assemblage characteristic of Mediterranean temperate woodland but with the appearance of *Mammuthus meridionalis* and *Equus stenonis* indicating a shift towards more open habitats. Pollen from the Dmanisi area (Messager et al., 2010, 2011) records the spread of temperate steppe-forest after the Olduvai normal excursion, with the vegetation dominated by herb taxa with steppic and xeric elements, indicating an increasing trend towards aridity as a result of the amplification of climatic oscillations at this time. The increasing presence of relatively dry and open environments favoured the expansion of herds of large herbivores that are likely to have played a key role in hominin subsistence (Dennell, 2003; Messager et al., 2010).

The time period suggested for the routing of the Gediz River through the palaeomeander section is time-equivalent to Marine Oxygen Isotope Stages 38—35 (see Lisiecki and Raymo, 2005, Fig. 5b). As there are no unequivocal palaeovegetation records covering this time period in Turkey, the nearest record for comparison is that from Tenaghi Philippon in north-eastern Greece (Tzedakis et al., 2006, Figs. 1, Fig. 5d). If we accept the age estimates, the Kale Tepe initial dam at ~1.24 Ma and the origins of the palaeomeander occur during the transition from MIS38 to MIS37, a time interval marked by a rapid rise in arboreal pollen taxa at

Tenaghi Philippon. Dense tree cover around Burgaz would have helped to stabilise the slopes above the meander section, allowing the river to erode freely into the Miocene basin fill without generating mass movement volumes capable of restricting lateral migration. The timing of the meander blockage falls within MIS35 after the Cobb Mountain sub-chron. It is possible that the majority of the infill of the abandoned palaeomeander is thus a product of slope instability during MIS34, as the proportion of slope-stabilising tree taxa falls sharply. A fragment of a lower molar of horse (*Equus* sp.) found within the slope sediment is consistent with the development of a more open habitat.

It is tempting to assign the occupation level to MIS 35, an exceptionally long interglacial. This prolonged period of relative climatic stability, taken together with the attractions of volcanic landscapes (Bailey and King, 2011), may have provided the perfect context for hominin dispersal across Anatolia.

Acknowledgements

Appendix A. Supplementary data

Supplementary data related to this article can be found at http://dx.doi.org/10.1016/j.quascirev.2014.11.021.

References

Bailey, G.N., King, G.C.P., 2011. Dynamic landscapes and human dispersal patterns: tectonics, coastlines, and the reconstruction of human habitats. Quat. Sci. Rev. 30, 1533—1553.

Bar-Yosef, O., Belmaker, M., 2011. Early and Middle Pleistocene Faunal and hominins dispersals through Southwestern Asia. Quat. Sci. Rev. 30, 1318—1337.

Biggin, A., van Hinsbergen, D.J.J., Langereis, C.G., Straathof, G.B., Deenen, M.H., 2008. Geomagnetic Secular variation in the Cretaceous Normal Superchron and in the Jurassic. Phys. Earth Planet. Inter. 169, 3—19.

Borsi, S., Ferrara, G., Innicenti, F., Mazzuoli, R., 1972. Geochronology and petrology of recent volcanics in the eastern Aegean Sea. Bull. Volcanol. 36, 473—496.

Bridgland, D.R., Saville, A., Sinclair, J.M., 1997. New evidence for the origin of the Buchan Ridge Gravel, Aberdeenshire. Scott. J. Geol. 33, 43—50.

Dankers, P.H.M., Zijderveld, J.D.A., 1981. Alternating field demagnetization of rocks, and the problem of gyromagnetic remanence. Earth Planet. Sci. Lett. 53, 89—92.

Deenen, M.H.L., Langereis, C.G., van Hinsbergen, D.J.J., Biggin, A.J., 2011. Geomagnetic secular variation and the statistics of palaeomagnetic directions. Geophys. J. Int. 186, 509—520.

Dennell, R., 2003. Dispersal and colonisation, long and short chronologies: how continuous is the Early Pleistocene record for hominids outside East Africa? J. Hum. Evol. 45, 421—440.

Dennell, R., 2008. Human migration and occupation of Eurasia. Episodes 31, 207—210.

Ersoy, Y., Helvacı, C., Sözbilir, H., 2010. Tectono-stratigraphic evolution of the NE—SW-trending superimposed Selendi basin: implications for late Cenozoic crustal extension in Western Anatolia, Turkey. Tectonophysics 488, 210—232.

Ferring, R., Oms, O., Agustí, J., Berna, F., Nioradze, M., Shelia, T., Tappen, M., Vekua, A., Zhvania, D., Lordkipanidze, D., 2011. Earliest human occupations at Dmanisi (Georgian Caucasus) dated to 1.85—1.78 mya. Proc. Natl. Acad. Sci. 108, 10432—10436.

Fisher, R.A., 1953. Dispersion on a sphere. Proc. R. Soc. Lond. A217, 295—305.

Gabunia, L., Vekua, A., 1995. A Plio-Pleistocene hominid from Dmanisi, east Georgia. Caucasus. Nature 373, 509—512.

Gabunia, L., Vekua, A., Lordkipanidze, D., Swisher III, C.C., Ferring, R., Justus, A., Nioradze, M., Tvalchrelidze, M., Antón, S.C., Bosinski, G., Jöris, O., Lumley, M., Majsuradze, G., Mouskhelishvili, A., 2000. Earliest Pleistocene hominid cranial remains from Dmanisi, Republic of Georgia: taxonomy, geological setting, and age. Science 288 (5468), 1019—1025.

Güleç, E., Howell, F.C., White, T.D., 1999. Dursunluda new lower Pleistocene artifact-bearing locality in southern Anatolia. In: Ullrich, H. (Ed.), Hominid Evolution: Lifestyles and Survival Strategies. Edition Archea, Berlin, pp. 349—364.

Güleç, E., White, T., Howell, F.C., Özer, I., Sağr, M., Yılmaz, H., Kuhn, S., 2009. The lower Pleistocene lithic assemblage from Dursunlu (Konya), central Anatolia, Turkey. Antiquity 83, 11—22.

Harmankaya, S., Tanındı, O., 1996. Türkiye Arkeolojik Yerleşmeleri, 1. Paleolitik/ Epipaleolitik, Istanbul: Ege Yayınları.

Hilgen, F.J., Lourens, L.J., van Dam, J.A., 2012. The Neogene period. In: Gradstein, F.M., Ogg, J.G., Schmitz, M.D., Ogg, G.M. (Eds.), The Geologic Time Scale 2012. Elsevier, pp. 923—978, 1144 pp.

Johnson, C.L., Constable, C.G., Tauxe, L., Barendregt, R., Brown, L.L., Coe, R.S., Layer, P., Mejia, V., Opdyke, N.D., Singer, B.S., Staudigel, H., Stone, D.B., 2008. Recent investigations of the 0—5 Ma geomagnetic field recorded by lava flows. Geochem. Geophys. Geosyst. 9, Q04032, 10.1029.2007GC001696.

Kirschvink, J.L., 1980. The least-squares line and plane and the analysis of palaeomagnetic data. Geophys. J. R. Astrol. Soc. 62, 699—718.

Kuhn, S.L., 2002. Paleolithic archaeology in Turkey. Evol. Anthropol. 11, 196—210.

Kuhn, S.L., 2010. Was Anatolia a bridge or a barrier to early hominin dispersals? Quat. Int. 223—224, 434—435.

Kuiper, K.F., Deino, A., Hilgen, F.J., Krijgsman, W., Renne, P.R., Wijbrans, J.R., 2008. Synchronizing rock clocks of earth history. Science 320, 500—504.

Lebatard, A.E., Cihat Alçiçek, M., Rochette, P., Khatib, S., Vialet, A., Boulbes, N., Bourlès, D.L., Demory, F., Guipert, G., Mayda, S., Titov, V.V., Vidal, L., de Lumley, H., 2014. Dating the Homo erectus bearing travertine from Kocabaş (Denizli, Turkey) at least 1.1 Ma. Earth Planet. Sci. Lett. 390, 8—18.

Lee, J.-Y., Marti, K., Severinghaus, J.P., Kawamura, K., Yoo, H.-S., Lee, J.B., Kim, J.S., 2006. A redetermination of the isotopic abundances of atmospheric Ar. Geochim. Cosmochim. Acta 70, 4507—4512.

Lisiecki, L.E., Raymo, M.E., 2005. A Pliocene-Pleistocene stack of 57 globally distributed benthic δ18O records. Paleoceanography 20, PA1003. http://dx.doi.org/10.1029/2004PA001071.

Lordkipanidze, D., Ponce de León, M.S., Margvelashvili, A., Rak, Y., Rightmire, G.P., Vekua, A., Zollikofer, C.P.E., 2013. A Complete skull from Dmanisi, Georgia, and the Evolutionary Biology of Early Homo. Science 342 (6156), 326—331.

McFadden, P.L., McElhinny, M.W., 1988. The combined analysis of remagnetisation circles and direct observations in paleomagnetism. Earth Planet. Sci. Lett. 87, 161—172.

Maddy, D., Demir, T., Bridgland, D., Veldkamp, A., Stemerdink, C., van der Schriek, T., Westaway, R., 2005. An obliquity-controlled Early Pleistocene river terrace record from Western Turkey? Quat. Res. 63, 339—346.

Maddy, D., Demir, T., Veldkamp, A., Bridgland, D.R., Stemerdink, C., van der Schriek, T., Schreve, D., 2012a. The obliquity-controlled early Pleistocene terrace sequence of the Gediz River, Western Turkey: a revised correlation and chronology. J. Geol. Soc. Lond. 169, 67—82.

Maddy, D., Veldkamp, A., Jongmans, A.G., Candy, I., Demir, T., Schoorl, J.M., van der Schriek, T., Stemerdink, C., Scaife, R.G., van Gorp, W., 2012b. Volcanic disruption and drainage diversion of the palaeo-Hudut River, a tributary of the Early Pleistocene Gediz River, Western Turkey. Geomorphology 165—166, 62—77.

Messager, E., Lordkipanidze, D., Delhon, C., Ferring, C.R., 2010. Palaeoecological implications of the Lower Pleistocene phytolith record from the Dmanisi site (Georgia). Palaeogeogr. Palaeoclimatol. Palaeoecol. 288, 1—13.

Messager, E., Lebreton, V., Marquer, L., Russo-Ermolli, E., Orain, R., Renault-Miskovsky, J., Lordkipanidze, D., Despriée, J., Peretto, C., Arzarello, M., 2011. Palaeoenvironments of early hominins in temperate and Mediterranean Eurasia: new palaeobotanical data from Palaeolithic key-sites and synchronous natural sequences. Quat. Sci. Rev. 30, 1439—1447.

Richardson-Bunbury, J.M., 1996. The Kula volcanic field, western Turkey: the development of a Holocene alkali basalt province and the adjacent normal-faulting graben. Geol. Mag. 133, 275—283.

Slimak, L., Kuhn, S., Roche, H., Mouralis, D., Buitenhuis, H., Balkan-Atlı, N., Binder, D., Kuzucuoğlu, C., Guillou, H., 2008. Kaletepe Deresi 3 (Turkey): archaeological evidence for early human settlement in central Anatolia. J. Hum. Evol. 54, 99—111.

Schneider, B., Kuiper, K., Postma, O., Wijbrans, J.R., 2009. 40Ar/39Ar geochronology using a quadrupole mass spectrometer. Quat. Geochronol. 4, 508—516.

Tzedakis, P.C., Hooghiemstra, H., Pälike, H., 2006. The last 1.35 million years at Tenaghi Philippon: revised chronostratigraphy and long-term vegetation trends. Quat. Sci. Rev. 25, 3416—3430.

Westaway, R., Guillou, H., Yurtmen, S., Beck, A., Bridgland, D.R., Demir, T., Rowbottam, G., 2006. Late Cenozoic uplift of western Turkey: improved dating and numerical modelling of the Gediz river terrace staircase and the Kula Quaternary volcanic field. Glob. Planet. Change 51, 131—171.

Westaway, R., Pringle, M., Yurtmen, S., Demir, T., Bridgland, D.R., Rowbottom, G., Maddy, D., 2004. Pliocene and Quaternary regional uplift in western Turkey: the Gediz river terrace staircase and the volcanism at Kula. Tectonophysics 391, 121—169.

Wijbrans, J.R., Pringle, M.S., Koppers, A.A.P., Scheveers, R., 1995. Argon geochronology of small samples using the Vulkaan argon laserprobe. Proc. Royal Neth. Acad. Arts Sci. 98, 185—218.

Wijbrans, J.R., Schneider, B., Kuiper, K., Calvari, S., Branca, S., De Beni, E., Norini, G., Corsaro, R.A., Miraglia, L., 2011. 40Ar/39Ar geochronology of Holocene basalts; examples from Stromboli, Italy. Quat. Geochronol. 6, 223—232.

Wymer, J., 1999. The Lower Palaeolithic Occupation of Britain, vols. 1 and 2. Wessex Archaeology and English Heritage, Salisbury.

Zijderveld, J.D.A., 1967. A.c. demagnetisation of rocks: analysis of results. In: Collinson, D.W., et al. (Eds.), Methods in Palaeomagnetism. Elsevier, Amsterdam, pp. 254—286.